CDF/ANAL/TOP/CDFR/6572
Version 1.0 , July 16, 2003

Search for Single Top Production at $\sqrt{\mathrm{s}} = 1.96$ TeV with CDF

Catalin Ciobanu[d], Pierre Savard[c], Bernd Stelzer[c], Evelyn Thomson[a], Thomas Müller[b], Wolfgang Wagner[b], Thorsten Walter[b]

[a] *Ohio State University, Columbus*
[b] *Universität Karlsruhe*
[c] *University of Toronto*
[d] *University of Illinois, Urbana-Champaign*

Abstract

We present first preliminary results of a search for single top quark production with CDF in Run II.

1 Data samples and event selection

For our analysis we use the high-p_T lepton (muon or electron) samples commonly used by the lepton+jets group. We apply the good run list distributed by the lepton+jets group which includes criteria to insure good data from the CDF silicon vertex detector. After applying the good run criteria we are left with 664179 events. The data include runs from no. 141544 to run no. 163527. These runs correspond to an integrated luminosity of $\int \mathcal{L}\, dt = (107.1 \pm 6.4)$ pb for central electrons (CEM) and muons triggered by the CMUP. The integrated luminosity for muons triggered by the CMX is $\int \mathcal{L}\, dt = (96.9 \pm 5.8)$ pb, since this subdetector went into operation later. The relative error on the luminosity measurement is 6%.

Our event selection was described in detail in a companion note [1]. Here we give only a brief summary:

1. We require one and only one standard tight lepton (electron or muon).

2. We require our events to pass the particular trigger path definition.

3. In muon data only (not in Monte Carlo) we apply the standard cosmic ray filter.

Cut	CEM	CMUP	CMX	All	N_i/N_{i-1}
All events				1046464	–
n Good Run				664179	63.47%
1 Tight Std. lepton	262981	45814	36605	345450	52.01%
Add ID cuts	223892	40003	24389	288284	83.45%
Trigger Path	221647	39698	24372	285717	99.11%
Conversion veto	122354	39698	24372	186424	65.25%
Z veto	117675	38393	23596	179664	96.37%
Cosmic veto	117675	38393	23596	179664	100%
Raw miss. Et (Info)	63877	30895	18625	113397	63.12%
Missing Et	63455	30815	18580	112850	62.81%
M_W real (Info)	53090	26298	15513	94901	84.09%
N tight jets ≥ 1 (I)	6134	2846	1612	10592	9.386%
miss tag (Info)	11	3	2	16	0.01418%
b tag ≥ 1	71	40	15	126	0.1117%
b tag $= 2$ (Info)	4	1	0	5	0.004431%
$E_T(\mathrm{b-jet}) > 15$ GeV	71	40	15	126	100%
b-Tag in lead. 2 jets (I)	70	39	14	123	97.62%
$2 \leq$ N Jet ≤ 2	20	13	7	40	31.75%
$140 \leq M_{b\ell\nu} \leq 210$	8	7	4	19	47.5%

Table 1: Cut flow of the event selection for single top events.

4. We use the standard conversion veto.

5. Standard Z boson rejection.

6. Missing transverse energy $\not\!\!E_T \geq 20$ GeV. We use jet corrections (level 3) to correct the $\not\!\!E_T$.

7. We require at least one SECVTX tagged jet. The tagging is applied to standard tight jets.

8. We count jets with corrected $E_T \geq 15$ GeV and $|\eta| < 2.8$. We require exactly 2 jets.

9. We reconstruct the invariant mass $M_{\ell\nu b}$ of the lepton, the $\not\!\!E_T$ (neutrino) and the b-jet. For signal events this quantity resembles the top quark mass. We require 140 GeV $\leq M_{\ell\nu b} \leq$ 210 GeV.

After applying all these cuts we observe 19 candidate events. Table 1 shows the cut flow for data. A listing of all 19 events is given in Table 14 in Appendix A.

1.1 Monte Carlo Samples

The Monte Carlo samples used in this analysis are listed in Table 2.

Sample	Process	Description	N events
ttop0s	t-ch.	Pythia, standard, no filter	512000
ttop1s	s-ch.	Pythia, standard, no filter	512000
ttop2s	t-ch.	Pythia, $m_{\rm top}$=170 GeV, ℓ filter	108719
ttop3s	t-ch.	Pythia, $m_{\rm top}$=180 GeV, ℓ filter	108821
ttop4s	s-ch.	Pythia, $m_{\rm top}$=170 GeV, ℓ filter	109673
ttop5s	s-ch.	Pythia, $m_{\rm top}$=180 GeV, ℓ filter	109853
ttop6s	t-ch.	Pythia, $m_{\rm top}$=175 GeV, ℓ filter	108754
ttop7s	s-ch.	Pythia, $m_{\rm top}$=175 GeV, ℓ filter	106876
ttop8s	t-ch.	Pythia, no ISR, ℓ filter	141553
ttop9s	s-ch.	Pythia, no ISR, ℓ filter	
ttop2i	$t\bar{t}$	Herwig, standard, no filter	390000
ttopcj	$t\bar{t}$	Herwig, $m_{\rm top}$=170 GeV, ℓ filter	
ttopfj	$t\bar{t}$	Herwig, $m_{\rm top}$=180 GeV, ℓ filter	
atop10	$We\nu b\bar{b}0p$	Alpgen	
atop16	$W\mu\nu b\bar{b}0p$	Alpgen	
atop13	$We\nu c\bar{c}0p$	Alpgen	
atop19	$W\mu\nu c\bar{c}0p$	Alpgen	
atop0w	$We\nu c0p$	Alpgen	
atop1w	$We\nu c1p$	Alpgen	
atop3w	$W\mu\nu c0p$	Alpgen	
atop4w	$W\mu\nu c1p$	Alpgen	

Table 2: Monte Carlo samples used in the single top analysis.

2 Event detection Efficiency and Expected Number of Events

2.1 Single Top signal and $t\bar{t}$ background

The determination of the event detection efficiency for single top t- and s-channel events as well as $t\bar{t}$ background events is described in a companion note [1]. We repeat our results in Table 3. We calculate the number of expected events according to

	t-channel	s-channel	$t\bar{t}$
ϵ^{CEM} [%]	0.431 ± 0.045	0.486 ± 0.049	0.175 ± 0.018
ϵ^{CMUP} [%]	0.226 ± 0.024	0.238 ± 0.025	0.092 ± 0.010
ϵ^{CMX} [%]	0.110 ± 0.012	0.132 ± 0.015	0.046 ± 0.006
$\sum_k \epsilon^k$ [%]	0.767 ± 0.052	0.857 ± 0.057	0.313 ± 0.022

Table 3: Summary of event detection efficiencies for t- and s-channel single top quark production and $t\bar{t}$ production. The numbers apply to the 2-jet bin only and include a cut on $M_{\ell\nu b}$.

$$N_j = \sigma_j \left(\left\{ \epsilon_j^{CEM} + \epsilon_j^{CMUP} \right\} \cdot \int \mathcal{L} dt^{CEM/CMUP} + \epsilon_j^{CMX} \cdot \int \mathcal{L} dt^{CMX} \right) \tag{1}$$

where σ_j is the theoretical cross section prediction for process j (t-channel single top, s-channel single top or $t\bar{t}$. We use the cross sections as described in in Ref. [1]. The resulting numbers of expected events for t- and s-channel single top quark production and $t\bar{t}$ evetns are given in Table 4. The uncertainties include the uncertainty of the prediction due to

Process	Cross Section	$\Delta\epsilon_{\mathrm{norm}}$	N Events	rel. uncert.
t-channel	(1.980 ± 0.24) pb	19.9%	1.61 ± 0.51	23.3%
s-channel	(0.884 ± 0.11) pb	19.4%	0.80 ± 0.18	23.0%
$t\bar{t}$	(6.70 ± 1.53) pb	20.0%	2.22 ± 0.67	30.0%

Table 4: Expected number of events for t- and s-channel single top production and the $t\bar{t}$ background.

1. the choice of the factorization and renormalization scale μ^2,
2. the top quark mass ($\Delta m = 5$ GeV),
3. the choice of the parton distribution function (PDF).
4. the uncertainty of 6% in the luminosity and
5. the uncertainty in the event detection effciency as given above.

For t- and s-channel we take the uncertainties as calculated in section 4. For $t\bar{t}$ we take a rough estimate of 20%.

2.2 Non-top background

In case of the non-top background we cannot use the same method to estimate the expected number of events as used for signal and $t\bar{t}$ because there are no reliable cross-section predictions. For the lepton+jets cross section measurement a background estimate was performed which is partly based in CDF data and partly on Monte Carlo simulations. Ideally, we have to redo this background estimate for our analysis. However, due to the tight time contraints we were not able to do that. Instead we use the background estimate for the lepton+jets cross section measurement and scale these numbers with the cut efficiencies for $M_{\ell\nu b}$ and the extended jet definition up to $|\eta| < 2.8$. Table 5 shows the assigned scale factors and the resulting number of background events. The scale factors

Process	$N_{\rm bkg}$ $(\ell + j)$	ϵ_η	ϵ_{lumi}	$N_{\rm bkg}(\lvert\eta\rvert < 2.8)$	$\epsilon_{M\ell\nu b}$	$N_{\rm bkg}(M_{\ell\nu b})$
$Wb\bar{b}$	3.9 ± 1.3	1.04	1.898	7.7 ± 3.4	0.45 ± 0.02	3.5 ± 1.5
$Wc\bar{c}$	1.5 ± 0.7	1.07	1.898	3.0 ± 1.7	0.45 ± 0.04	1.4 ± 0.8
Wc	3.4 ± 0.9	1.15	1.898	7.4 ± 2.3	0.42 ± 0.02	3.1 ± 1.0
Mistags	2.9 ± 0.33	1.11	1.898	6.1 ± 1.9	0.47 ± 0.07	2.9 ± 0.9
non-W	2.4 ± 0.6	1.15	1.898	5.2 ± 1.5	0.42 ± 0.06	2.2 ± 0.7
Diboson	0.8 ± 0.2	1.03	1.898	1.6 ± 0.5	0.46 ± 0.05	0.7 ± 0.2
$Z + b\bar{b}$	0.08 ± 0.03	1.04	1.898	0.16 ± 0.06	0.45 ± 0.02	0.07 ± 0.03
Sum	15.0 ± 2.4	–	–	31.2 ± 6.2	–	13.8 ± 2.8

Table 5: Estimates of non-top background evetns. The second column gives the number of background events estimated for the lepton+jets cross-section measurement using 57.5/47.3 pb^{-1} of data. The errors on $\epsilon_{M\ell\nu b}$ are purely statistical.

for $Wb\bar{b}$, $Wc\bar{c}$, Wc and di-boson events were obtained from the corresponding Monte Carlo samples. For di-boson events we evaluated Monte Carlo samples with with WW, WZ and ZZ events. The individual numbers for the $M_{\ell\nu b}$ cut are: 44.3% for WW, 47.4% for WZ and 57.4% for ZZ. We calculated the weighted averaged using the predicted cross-sections for these processes as weight. The result is 45.8%, which we round up to 46%.

To "Mistags" we assigned a scale factor by looking at untagged W+jet events. For $Z + b\bar{b}$ we used the scale factor of $Wb\bar{b}$. For the non-W background and the we use the biggest occuring factor, i.e. the one from Wc (for ϵ_η) and for "Mistags" (for $M_{\ell\nu b}$. We assign a systematic error of 3% to the scale factor to ϵ_η.

The lepton+jet numbers are for an integrated luminosity of 57.5/47.3 pb^{-1}. To get the background numbers for 107.1/96.9 pb^{-1}. We scale up by a factor ϵ_{lumi}. Here we have to take the relative acceptances of CEM/CMUP and CMX into account. For $Wb\bar{b}$ events this ratio is 0.81/0.19. We therefore use: $\epsilon_{lumi} = 107.1/57.5 \cdot 0.81 + 96.9/47.3 \cdot 0.19 = 1.898$. We use this number for all processes.

Two background estimates for $Wb\bar{b}$, $Wc\bar{c}$ and mistags were performed in the lepton+jet cross section measurement. They are genericly called "Method 1" and "Method 2". Method 1 is entirely based on the mistag matrix and generally believed to overestimate the bnackground. That's why we used the "Method 2" results in Table 5. In the

Process	N Events
t-channel	1.61 ± 0.51
s-channel	0.80 ± 0.18
$t\bar{t}$	2.22 ± 0.67
non-top	13.8 ± 2.8
Sum	18.43 ± 2.93

Table 6: Summary table of the expected number of events.

2-jet bin "Method 1" and "Method 2" give quite different results, e.g. for 57.5 pb^{-1}: 12.4 versus 8.4 events. To cover this uncertainty we attribute half of the difference between the two methods as a systematic uncertainty in our background estimate, i.e. we add an uncertainty of 23.8% for $Wb\bar{b}$, $Wc\bar{c}$ and mistags.

2.3 Summary: Expected Events

Table 6 summarizes the number of expected events used in our likelihood fit. The number of signal events serves as a normalization and as start value for Minuit. The number of background events and their errors are used to constrain the fit.

3 Feldman-Cousins Counting Limits

Our analysis uses a likelihood fit to determine the signal and background fractions in the data. However, it is instructive to compute a confidence interval merely based on the number of oberserved events N and number of expected background events B. For this purpose we use Feldman-Cousins confidence intervals. For the calculation we use a little program developed by J.A. Aguilar-Saavedra [2]. The number of observed candidate events is $N = 19$.

For the combined limit we use $B = 16$. The resulting confidence interval is $[0.00,\ 13.31]$ (Number of events). Normalizing to the number of expected signal events $N_{\text{exp}} = 2.41$ we get $\beta_{95} = 5.52$. This corresponds to a cross-section limit of $\sigma < 15.8$ pb at 95% C.L..

For the separate limits on t- and s-channel we use $B_t = 16.8$ and $B_s = 17.6$. We get confidence intervals of $[0.00,\ 12.51]$ and $[0.00,\ 11.70]$, respectively. This leads to $\beta_{95}(\mathrm{t-channel}) = 7.77$ and $\sigma_t < 15.4$ pb at 95% C.L.. For the s-channel we get $\beta_{95}(\mathrm{s-channel}) = 14.63$ and $\sigma_s < 12.9$ pb at 95% C.L..

4 Systematic Uncertainties

This section discusses the systematic uncertainties on the signal normalization. We have to consider several sources of uncertainties:

1. Uncertainty due to the jet energy scale.

2. Uncertainty due to the modelling of initial and final state radiation.

3. Uncertainty due to the choice parton distribution functions.
4. Uncertainty due to the signal generator PYTHIA versus other signal generators.
5. Uncertainty in the top quark mass ($\Delta m = 5$ GeV).
6. Uncertainty in the b-tagging efficiency.
7. Uncertainty in the trigger and lepton id efficiency.

4.1 Jet Energy Scales

We have investigated the uncertainty on the jet energy scale by using the member function in the JetEnergyCorrection class which varies the jet energy scale by one sigma. The resulting deviations are given in Table 7 in percent. To cover the normalization uncertainty

	CEM	CMUP	CMX	All
t-channel				
$N_{\text{jet}} = 2$	-0.29%/-4.59%	-0.05%/-3.0%	-1.68%/-4.8%	-0.41%/-4.1%
$M_{l\nu b}$	-4.11%/-7.11%	-2.9%/-4.44%	-3.74%/-10.13%	-3.66%/-6.65%
s-channel				
$N_{\text{jet}} = 2$	-4.09%/-1.33%	-3.51%/-1.05%	-3.82%/-2.15%	-3.87%/-1.37%
$M_{l\nu b}$	-7.55%/0%	-8.25%/-1.37%	-4.36%/-0.94%	-7.272%/-0.57%

Table 7: The uncertainty due to the jet energy scale for t- and s-channel single top quark production.

due to the jet energy scale we assign systematic errors of 6.7% to the t-channel and 7.3% to the s-channel. This covers the maximum changes seen in Table 7.

4.2 Top Mass Uncertainty

To investigate the influence of the top quark mass on our signal acceptance we generated single top events for different masses: 170 and 180 GeV. Since we used a different version of the runMC executable than before and we used a lepton filter, we also generated the regular signal samples for 175 GeV. Table 8 shows the Monte Carlo event counts after all cuts. Since the samples have different sizes we calculate a normalized number of event N_{norm} which is normalized to the number of events in the samples for $m_{\text{top}} = 175$ GeV. Three out of four deviations are statistically compatible with zero. We assign the maximum relative deviation as a systematic error: t-channel 5.3%, s-channel 1.0%.

	t-channel				s-channel			
m_{top}	Sample	Events	N_{norm}	Devia.	Sample	Events	N_{norm}	Devia.
170	ttop2s	3401	3402.1	+0.1%	ttop4s	3225	3142.8	+1.0%
175	ttop6s	3398	3398	–	ttop7s	3113	3113	–
180	ttop3s	3579	3576.8	+5.3%	ttop5s	3182	3095.8	-0.6%

Table 8: Event counts of single top quark Monte Carlo samples for different top masses. The relative statistical error on these numbers is about 1.8%. We also give the relative deviation from the value for $m_{\text{top}} = 175$ GeV. Three out of four deviations are statistically compatible with zero.

Process	Sample	Events	N_{norm}	Devia.
t-channel	ttop8s	4998	3839.9	+13%
s-channel	ttop9s	6224	3656.8	+17.5%

Table 9: Event counts of single top quark Monte Carlo samples if initial state radiation is turned off.

4.3 Initial and Final State Radiation

At present there exists no realistic way to estimate uncertainties due to the modelling of ISR and FSR radiation in the Monte Carlo. Releastic would be to use two different modells which represent a reasonable range. Instead we generated Monte Carlo events were ISR was completely switched off (ttop8s and ttop9s). The event yields of these samples are given in Table 9. For modelling ISR we assign half the difference between ISR on and off as systematic error.

4.4 Summary on Systematic Uncertainties

Table 10 summarizes the systematic uncertainities on the signal normalization. The error on the event detection efficiency includes the trigger, lepton id and b-tagging errors.

	Relative Uncertainty		
Source	t-channel	s-channel	combined
Jet energy scale	6.7%	7.2%	6.9%
ISR	6.5%	8.7%	7.2%
FSR	7%	5%	6%
PDF	5%	5%	5%
Generator	10%	10%	10%
Top quark mass	5.3%	1.0%	4.0%
$\epsilon_{\rm evt}$	10.6%	10.4%	10.5%
luminosity	6%	6%	6%
Quadratic Sum	20.9%	20.6%	20.6%

Table 10: Summary table on systematic uncertainties on the event detection efficiency and luminosity.

5 Search for t-Channel Single Top Quark Production

A very distinct signature of t-channel single top quark production is a light-quark jet in the forward direction at high pseudo-rapidities. If a top quark is produced, the light quark jets has higher probability to be at high positive η. If an anti-top quark is produced, the light quark jet is more probable to be at high negative η. Therefore, the quantity $Q\,\eta$, where Q is the charge of the high-p_T lepton coming from the W decay is a good quantity to isolate the t-channel production mode. Fig. 1 shows the $Q\,\eta$ for t- and s-channel single top quark production, $t\bar{t}$

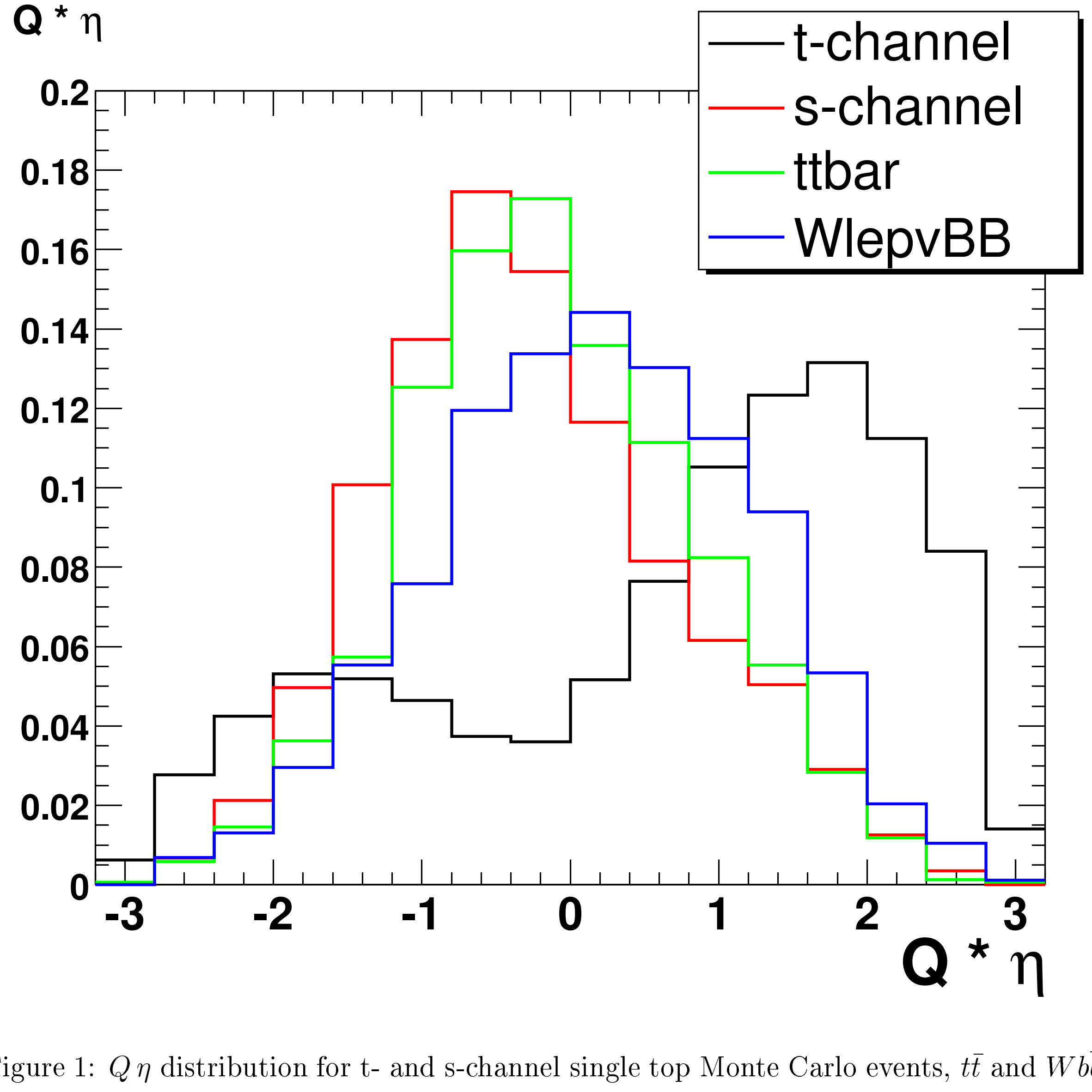

Figure 1: $Q\,\eta$ distribution for t- and s-channel single top Monte Carlo events, $t\bar{t}$ and $Wb\bar{b}$ events.

5.1 The Likelihood Function

We use a binned likelihood fit determine the sample composition. We constrain the two background samples to their standard model expectations by adding Gaussian constrains to the likelihood function.

To easier compare different sets of pseudo-experiments with each other we introduce the variable $\beta_j = n_j/\nu_j$ where n_j is the number of events of process j contained in the data and ν_j is the expected number of events according to theoretical predictions (single top and $t\bar{t}$) or experimental estimates (non-top background).

$$L = G_{t\bar{t}}(\mu_{t\bar{t}}, n_{t\bar{t}}, \sigma_{t\bar{t}}) \cdot G_{nt}(\mu_{nt}, n_{nt}, \sigma_{nt}) \cdot G_{all}(\mu_{all}, n_{all}, \sigma_{all}) \prod_{k=1}^{B} \frac{e^{-\mu_k \cdot \mu_k^{n_k}}}{n_k!}$$

The Gaussian constraints to the background are given by:

$$G_j(\beta_j; \nu_j, m_j, \sigma_j) = \frac{1}{\sigma_j \cdot \sqrt{2\,\pi}} \exp\left[-\frac{1}{2} \cdot \left(\frac{\beta_j\, \nu_j - m_j}{\sigma_j} \right)^2 \right]$$

$$\mu_k = \beta_{\mathrm{tch}}\, \nu_{\mathrm{tch}}\, \alpha_k + \beta_{\mathrm{sch}} \cdot \nu_{\mathrm{sch}}\, \gamma_k + \beta_{\mathrm{t\bar{t}}} \cdot \nu_{\mathrm{t\bar{t}}} \kappa_k + \beta_{\mathrm{nt}} \cdot \nu_{\mathrm{nt}}\, \rho_k$$

The index k runs over the bins of the fitted histogram. The quantities α_k, γ_k, κ_k and ρ_k are the bin contents of the normalized histogram for the different processes.

When fitting data to the Gaussian constraints use $m_j = \nu_j$. When fitting pseudo-experiments m_j is smeared with a Gaussian of width σ_j.

5.2 Fitter Performance

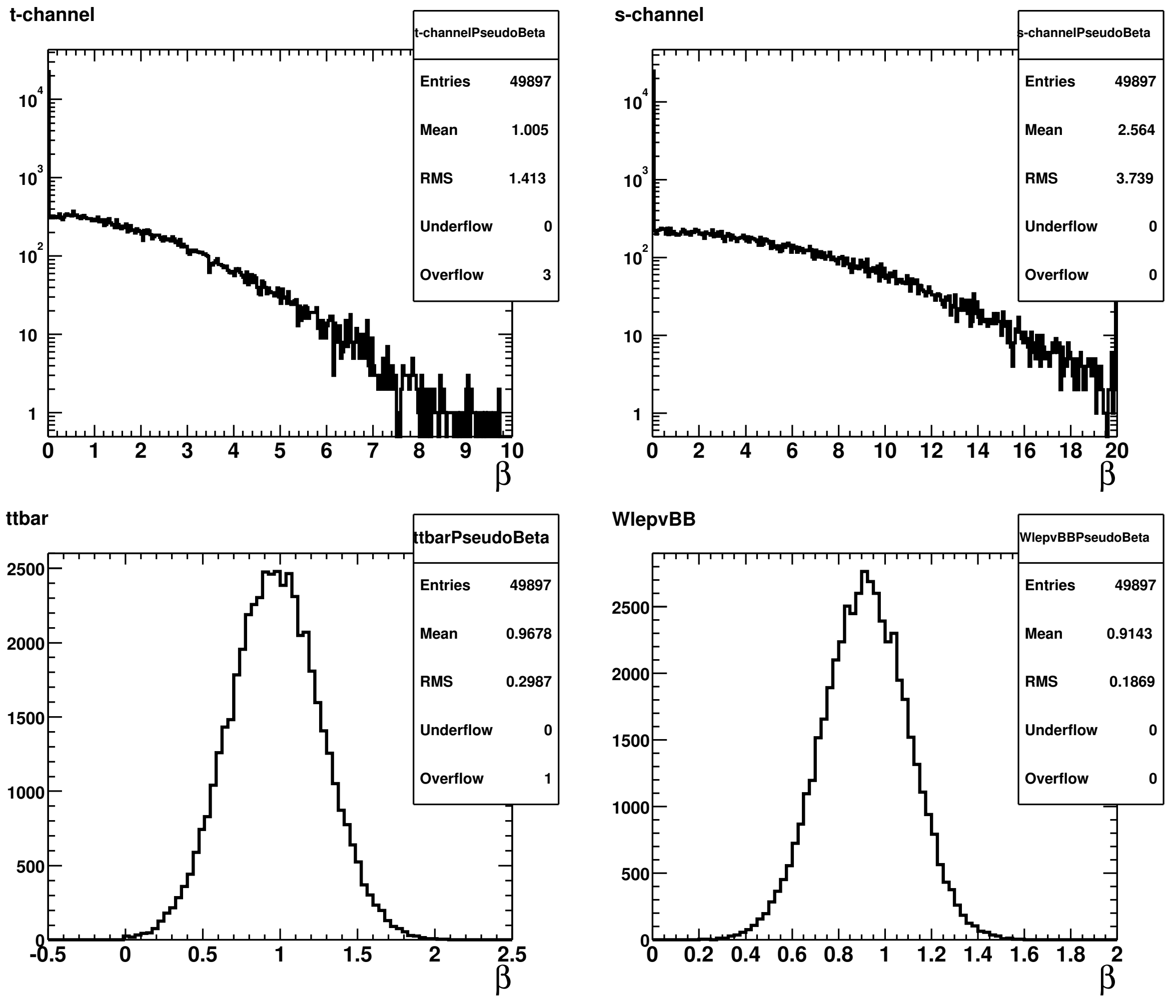

Figure 2: β distribution of 49897 pseudo-experiments for 107 pb^{-1} of data. β is the number of events returned by the fit over the exepctation. In case of pseudo-experiments the number of expected events is used as input.

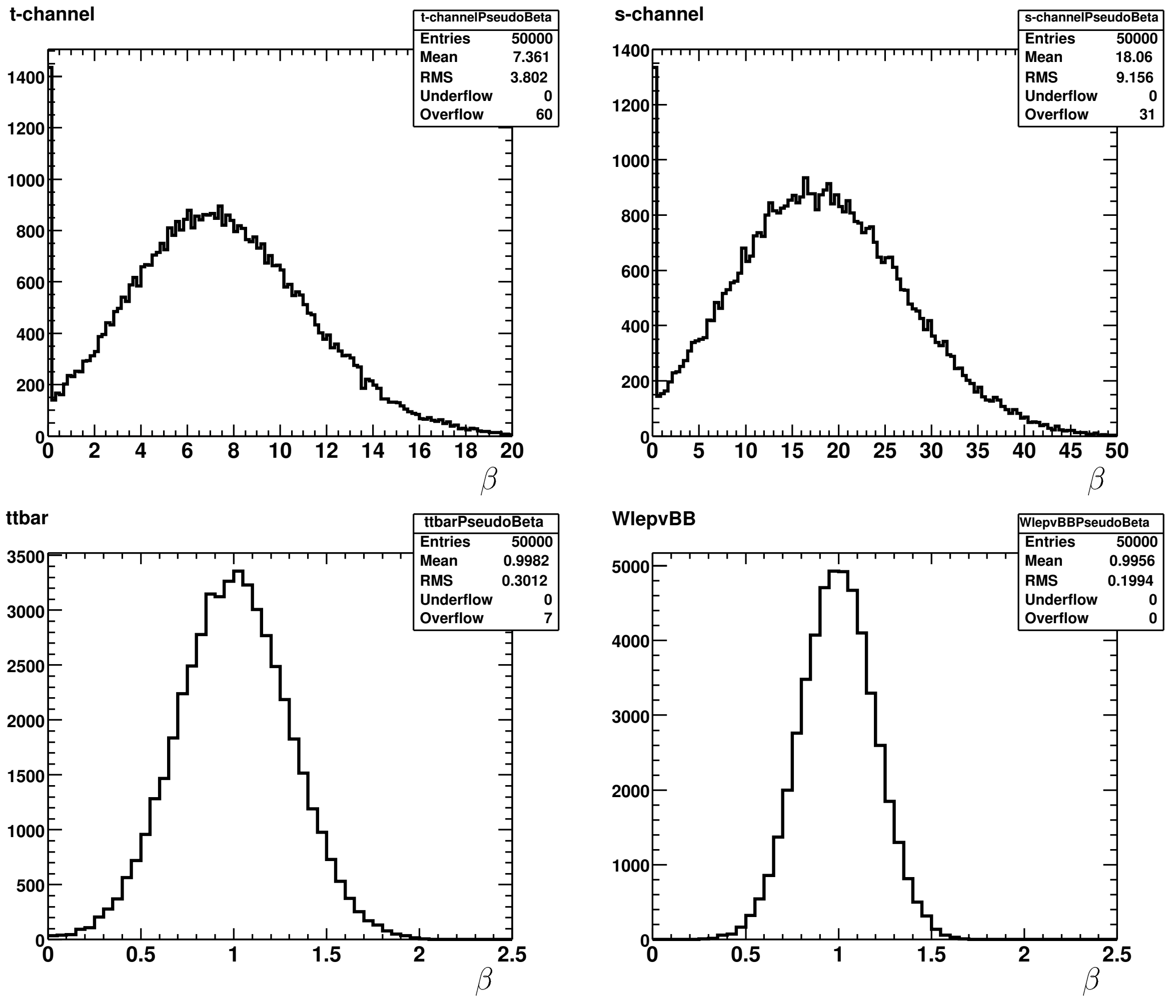

Figure 3: β distribution of 50000 pseudo-experiments used to set the a priori limits for the t- and s-channel search.

Source	Uncertainty	
	t-channel	s-channel
ISR	6.8%	3.0%
Top Mass	6.7%	2.5%
Jet Energy Scale	21.5%	8.3%
Background Model	43%	14.3%
Sum	49%	17%

Table 11: Systematic uncertainties from the likelihood fit (shape uncertainties).

5.3 Systematic Fit Uncertainties

The sources of systematic uncertainties listed in section 4 not only influence the absolute normalization of the signal via the acceptance but also influence the $Q\,\eta$ distribution used in the maximum likelihood fit. We investigate the size of these uncertainties in this section. We call this uncertainty the shape uncertainty.

We investigate the shape uncertainties by using specific Monte Carlo samples as described in section 4, e.g. with different top mass, ISR switched off or different signal generator. We construct pseudo-experiments from these "systematic" samples and fit these to the standard templates. The difference in the mean between the standard pseudo-experiments and those involving a systematic effect is used as an estimator of the systematic uncertainty for a specific source. Table 11 lists the shape uncertainties of the different sources.

5.4 Fit the Data

The fit results are listed in Table 12.

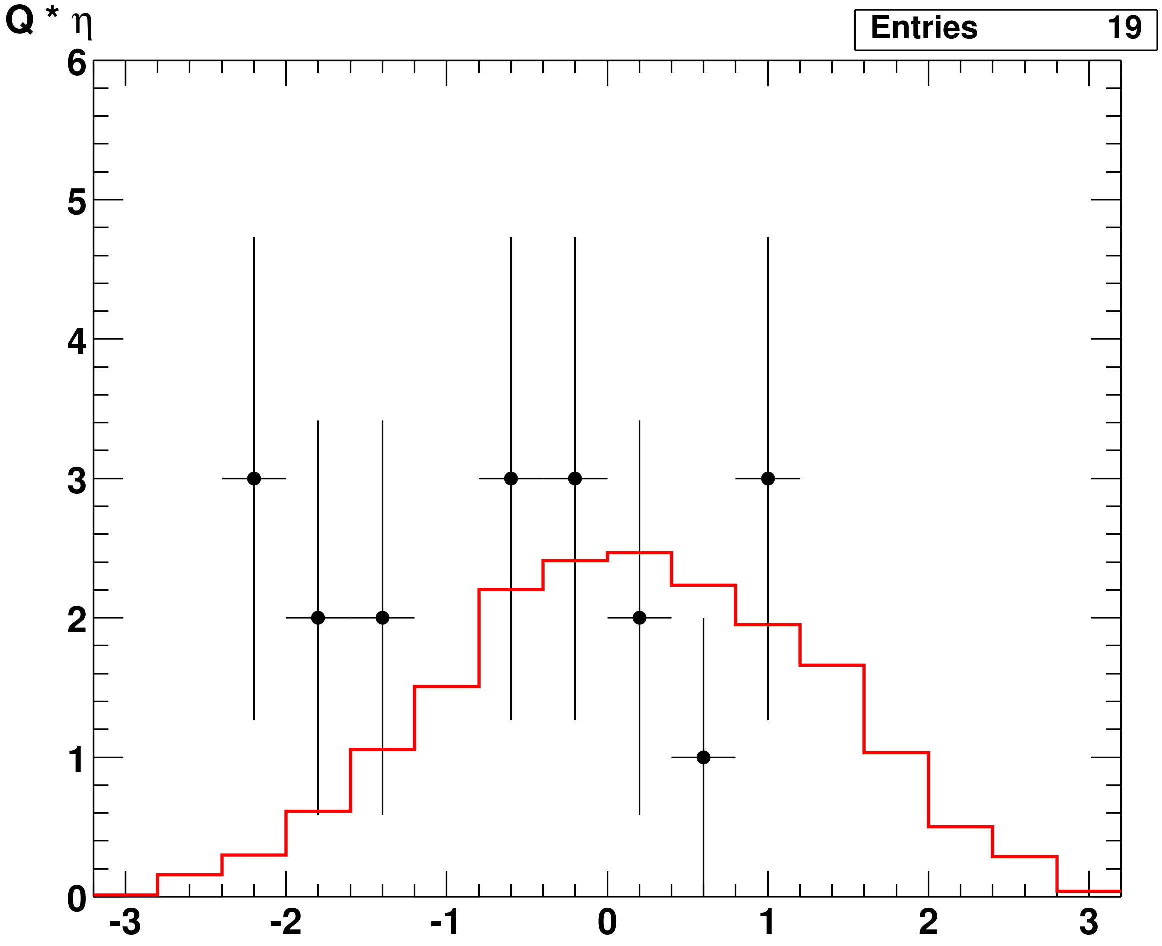

Figure 4: $Q\,\eta$ distribution for data (dots with error bars) and the fit result (line histogram).

Process	β_{fit}	n Events
t-channel	0.0 ± 2.6	0.0 ± 4.2
s-channel	5.6 ± 3.5	4.5 ± 2.8
$t\bar{t}$	0.98 ± 0.30	2.17 ± 0.7
$Wb\bar{b}$	0.90 ± 0.19	12.4 ± 2.7
Sum	–	19.03

Table 12: Fit results for 19 candidate events.

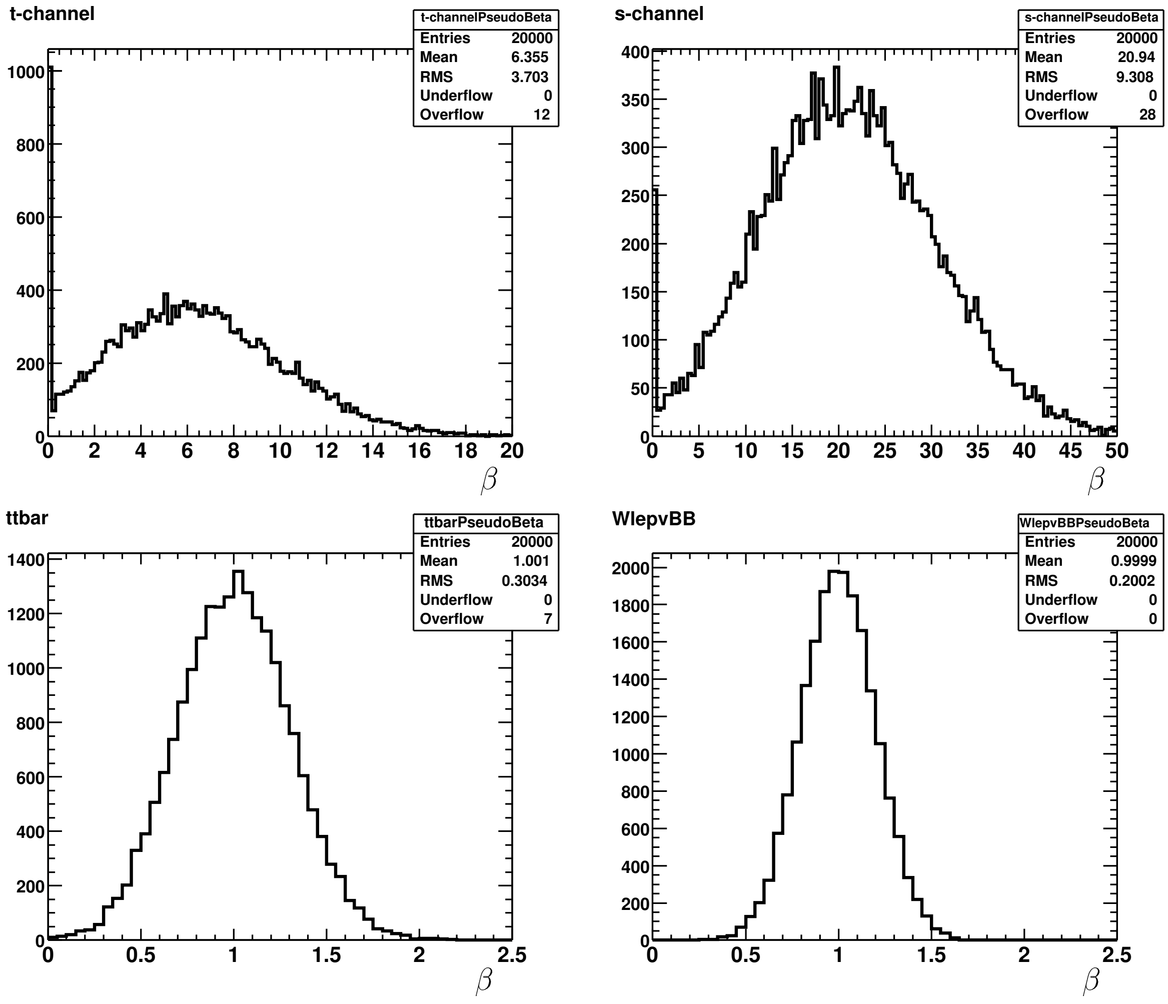

Figure 5: β distribution of 20000 pseudo-experiments used to set the a posteriori limit for the t- and s-channel search.

5.5 Bayesian Limit

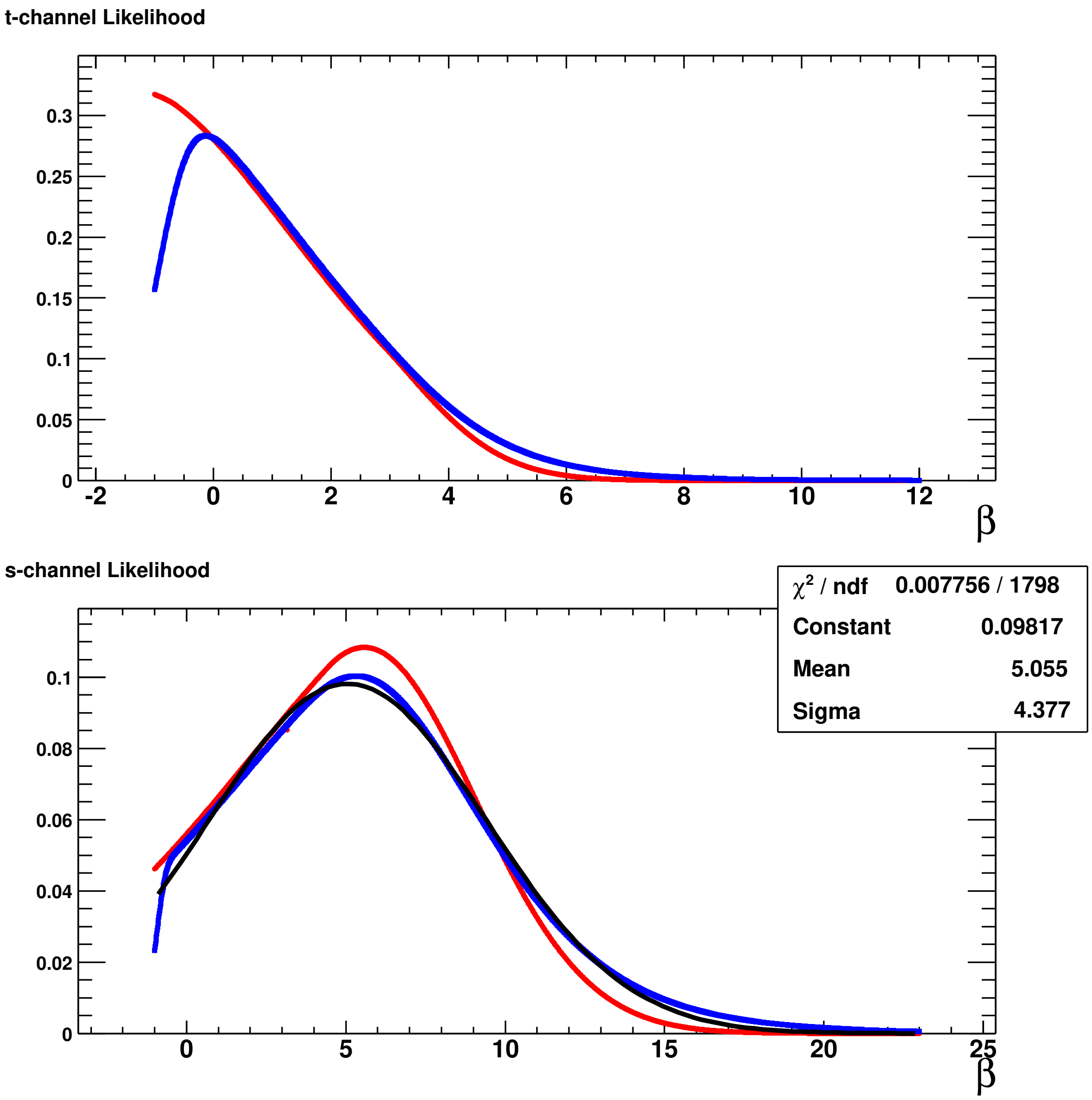

Figure 6: Likelihood function for t- and s-channel. Red curve without, blue curve with smearing according to the systematic errors. The black curve is a Gauss fit to the likelihood function.

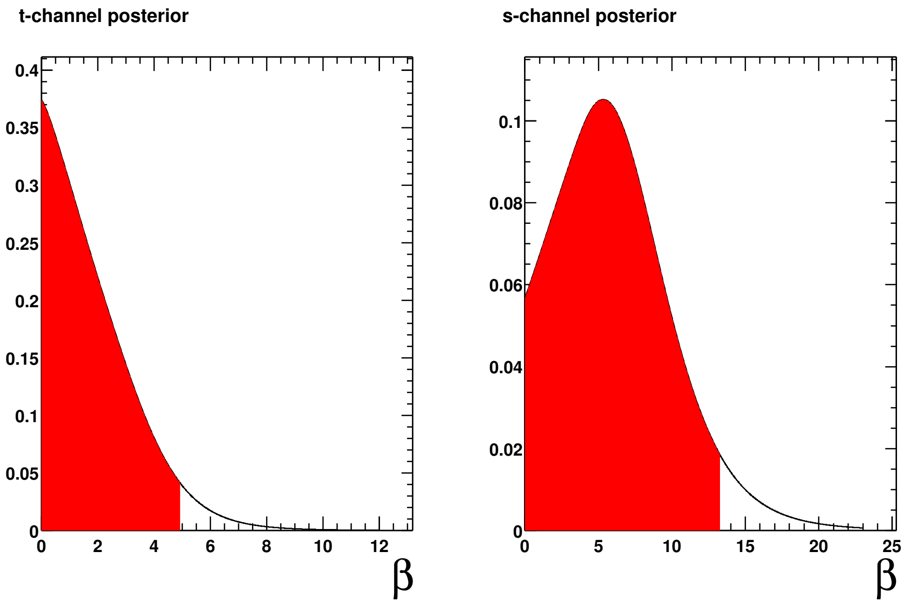

Figure 7: Bayesian posterior probability density function. The underlying likelihood function was smeared according to the systematic errors.

Process	t-channel	s-channel
A priori limit		
β_{95}	7.41	17.93
σ_{95}	14.7 pb	15.9 pb
Fit to the data		
β_{data}	0.0 ± 2.6	5.6 ± 3.5
N_{data}	0.0 ± 4.2	4.5 ± 2.8
Frequentist a-posteriori limit		
β_{95}	6.375	21.0
σ_{95}	12.6 pb	18.6 pb
Bayesian limit – no sys. errors		
β_{95}	4.20	11.33
σ_{95}	8.3 pb	10.0 pb
Bayesian limit – with sys. errors		
Δ_{norm}	20.9%	20.5%
Δ_{shape}	49.0%	20.0%
β_{95}	5.04	13.5
σ_{95}	10.0 pb	11.9 pb

Table 13: Cross-section limits for t- and s-channel

Appendix A: Event listing

Run No.	Event No.	Lepton	$\not\!\!E_T$ / GeV	$M_{\ell\nu b}$ / GeV
141621	249957	e	28.03	142.40
148856	250809	e	54.73	159.37
148916	792764	e	53.95	204.44
149355	635452	μ	42.29	209.63
149387	3663657	μ	52.59	191.05
150799	782782	μ	68.44	178.29
151434	754793	μ	60.00	203.85
153389	361345	e	28.85	167.45
154654	3709294	e	17.01	152.92
155365	79584	μ	45.62	171.21
155818	1980579	μ	64.72	141.96
156006	1299738	e	59.29	145.28
160988	2066916	μ	38.12	174.35
161552	522397	μ	40.49	154.56
161678	3946514	μ	76.14	158.64
162479	626796	μ	50.93	173.95
162498	7098336	e	53.51	204.57
162857	8321209	e	31.02	148.90
163064	4878884	μ	66.06	191.21

Table 14: Listing of 19 candidate events selected in our single top analysis.

References

[1] C. Ciobanu et al., CDF Note 6508, *Single Top Acceptance in Run II at CDF.*

[2] J.A. Aguilar-Saavedra, Comp. Phys. Com. 130 (2000) 190–203.